Segmentation of Brain Tumours in MR Images

Paweł Szwarc, *Silesian University of Technology*

Abstract

The paper deals with the segmentation of brain tumours in magnetic resonance (MR) images. The segmentation method developed is based on the analysis of two MR series, namely contrast enhanced T1-weighted images with gadolinium contrast medium and perfusion maps. The T1-weighted images are segmented using the Kernelised Weighted C-Means (KWCM) method, yielding a binary mask of candidates of the tumour tissue. Next, these results are compared with the perfusion intensity of the segmented regions and then with corresponding areas on the opposite side of the brain. The results obtained for subjects with glioblastoma multiforme (GBM) and anaplastic astrocytoma (AA) are discussed.

1. Introduction

Brain tumours remain one of the most difficult tumours to be treated as they often attack areas where the treatment of choice namely the total tumour resection is virtually impossible. Correct decisions concerning surgery, radiotherapy and chemotherapy planning depend firmly on the accurateness of tumour segmentation performed by a specialised radiologist. This work done manually by the radiologist is a tedious and time-consuming task.

The aim of this research is to create an automatic algorithm that may be an extremely helpful tool for radiologists assisting them in brain tumours segmentation in MR images.

1.1 Brain Tumours

Intracranial brain tumours are divided into two groups depending on the origin of cells building them: intraaxial and extraaxial tumours. Most of the intraaxial tumours are built from glial cells. These tumours called gliomas constitute some 50% of all brain tumours. Mostly gliomas are built of astrocytal cells. These tumours comprising some 35% of all brain tumours are called astrocytomas. The glioblastoma multiforme (GBM) is an astrocytoma tumour, classified by the World Health Organisation as having the highest IVth grade of malignancy (WHO IV) and thus being one of the most aggressive tumours. The GBM's constitute one fifth of all brain tumours [1]. The anaplastic astrocytoma is a WHO III astrocytoma, accounting for about 4% of all brain tumours [14].

These tumours are histologically very weakly delimited from healthy tissue. Necrosis, haemorrhage into the lesion and tumour angiogenesis are often to be encountered. Extended edema is also frequently diagnosed. These characteristics make the proper delineation of high-grade astrocytomas boundaries a laborious and difficult task [1].

The reoccurring tendency of GBM's even after radical resection and intensive radio- and chemotherapy treatment results in very poor survival rates, with median survival rate with and without treatment of ca. 3 and 8 months respectively and the 3-year survival rate after GBM diagnosis being as small as 2% [1, 19]. The median survival rate for subjects with anaplastic astrocytomas ranges from 2 to 5 years [15].

Nevertheless new treatment methods are tested and introduced, their efficiency being dependent on the correct tumour segmentation and quantification of its volume, which makes the assistance in the radiologists' task of the GBM segmentation process in MR images extremely vital.

1.2 The Nature of Magnetic Resonance Imaging (MRI) Data

The MRI data, dealt with in this research, include two MRI series of subjects with diagnosed GBM or anaplastic astrocytoma, namely T1-weighted images after the injection of gadovist contrast medium and perfusion maps obtained on the basis of Perfusion-Weighted Imaging (PWI) series by means of manufacturer's software. The images were made on a 3.0T Phillips MR appliance and a 1.5T Siemens MR appliance. Both imaging series are transverse-type and were made with the same angle positioning in coronal and saggital planes. All the subjects have undergone radical tumour resection as well as radio- and chemotherapy treatment.

The use of gadovist contrast medium allows to separate the regions of broken brain blood barrier. The enhancement of signal intensity, resulting from the shortening of the T1 time and caused by the

accumulation of gadolinium compounds, is best to be noticed in T1-weighted images. This signal intensity enhancement does not however necessarily mean by itself that the lesion is malignant [1]. The irregular, ring-shaped signal intensity enhancement, characteristic for GBM's [2], is well to be noticed in most of the images.

PWI plays an important role in treating primary brain tumours, as it makes it possible to find the most cancerous part of the tumour. It seems that the enhancement of the relative cerebral blood volume (RCBV), whose amount is represented by the image intensity level of the perfusion maps in the lesion area is caused by tumour angiogenesis, which may indicate the grade of malignancy of the tumour [1].

The RCBV coefficient is also helpful in telling the actual tumour areas from the radionecrosis areas and postoperative granulation tissue, all of them being hyperintensive in T1-weighted images after contrast medium administration.

The midline structures are often displaced due to an expansive lesion which makes it difficult to correctly establish the brain symmetry line in MR images. The brain symmetry itself may also often be disturbed by the tumour due to the mass efect [1].

1.3 Previous Attempts at Brain Tumour Segmentation

Most of the previous attempts at brain tumour segmentation are researches on automatic segmentation algorithms, although semi-automatic methods are also common. However, none of the researches has yet succeeded in creating universal software able to facilitate the segmentation of all kinds of brain tumours, the difficulty of the problem lying mainly in the variety of shapes and locations of brain tumours.

As far as semi-automatic brain tumours segmentation methods are concerned, the most widespread algorithms are defined respectively as seeded region growing and active contours and are dealt with for T1-weighted contrast images e.g. in [3].

In that research the seeded region growing algorithm is applied based on the extraction of a connected set of pixels whose intensities are consistent with the pixel statistics of the seed point chosen by the user. In the active contours algorithm the geodesic deformable model provided by [4] and the geometric active contours method based on the theory of curve evolution were implemented [3].

Among automatic brain tumour segmentation algorithms the most common are the Gaussian Mixture Models (GMM), the Support Vector Machine (SVM) and the Fuzzy C-Means (FCM) methods.

One-class SVM was developed to separate tumour and non-tumour regions in [5]. Structural analysis-based tumour segmentation scheme was presented in [6]. Firstly, three kind of features including those intensity-based, symmetry-based and texture-based were extracted from structural elements. Then a classification technique using the AdaBoost algorithm was suggested to classify the structural elements into normal and abnormal tissues. The authors of [7] presented GMM and SVM-based methods for brain segmentation.

2. Segmentation Algorithm

The Multiple Sclerosis (MS) Computer Aided Diagnosis (CAD) software created originally for the segmentation of demyelination plaques in brain MR images and described in [8] was applied for the segmentation of contrast enhanced areas in T1-weighted images. The basic algorithm, permitting the segmentation of white matter, brain matter and contrast enhanced areas, implemented in this software, is the Kernelised Weighted C-Means (KWCM). This method emerged directly from the standard Fuzzy C-Means (FCM) method [9, 10].

FCM is a clustering method based on the minimisation of an objective function. It divides a finite collection of elements into c clusters with respect to some given criterion [10, 17]. The data clustering methods using kernel functions allow a nonlinear transposal of the data into a high-dimensional space. The KWCM method fully transposes the clustering process into that high-dimensional space [11, 12]. The Radial Basic Function (RBF) is used as kernel function for the KWCM algorithm in the software. The feature incorporated in the clustering process is the signal intensity.

The FCM objective function for partitioning a dataset $X = \{x_1, x_2, ..., x_i, ..., x_N\}$ into c clusters can be defined as [10]

$$J(U) = \sum_{k=1}^{c} \sum_{i=1}^{N} u_{ki}^{\beta} d_{ki} , \qquad (1)$$

β being the fuzzyfication parameter, d_{ki} the distance measure selected between the i th object and the k th cluster centre and u_{ki} the elements of U - the fuzzy partition matrix.

In each iteration of the FCM algorithm, for each cluster k, the fuzzy cluster centre [17]

$$v_k^{(t)} = \frac{\sum_{i=1}^{N} (u_{ki})^{\beta} x_i}{\sum_{i=1}^{N} (u_{ki})^{\beta}} \qquad (2)$$

is calculated using fuzzy membership values in the partition matrix $U^{(t)}$. In the first iteration $U^{(1)}$ as well as the cluster centres are set to random values.

In the next steps $U^{(t+1)}$ values are recomputed following the equation [17]

$$u_{ki}^{(t+1)} = \frac{1}{\sum_{j=1}^{c} (d_{ki} / d_{ji})^{\frac{1}{\beta-1}}}, \quad (3)$$

where d denotes the distance metric selected. If the selected norm $\left\| U^{(t+1)} - U^{(t)} \right\| \le \varepsilon$, the computations stop and the defuzzyfication makes the analysed data x_i belong to the class k, if the u_{ki} fuzzy memebrship value is the highest of all $u_{ji} (j = 1,...,c)$ values.

The Kernelised Fuzzy C-Means (KFCM) algorithm adopts a kernel-induced distance metric, the objective function being [18]

$$J(U,\phi) = \sum_{k=1}^{c} \sum_{i=1}^{N} u_{ki}^{\beta} \left\| \phi(x_i) - \phi(v_k) \right\|^2, \quad (4)$$

with ϕ denoting a nonlinear mapping function into a higher dimensional feature space.

Substituting the Gaussian RBF

$$\phi_G(x, y) = \exp(-\|x - y\|^2 / \sigma^2) \quad (5)$$

as the kernel function and bearing in mind that $\phi_G(x,x) = 1$, equation (4) can be simplified to

$$J(U,\phi) = 2\sum_{k=1}^{c} \sum_{i=1}^{N} u_{ki}^{\beta} (1 - \phi_G(x_i, v_k)). \quad (6)$$

Taking the first derivative of $J(U,\phi)$ with respect to u_{ki} and comparing it to zero yields the following equation for the fuzzy partition matrix values [18]

$$u_{ki}^{(t+1)} = \frac{(1 - \phi_G(x_i, v_k))^{\frac{-1}{\beta-1}}}{\sum_{j=1}^{c} (1 - \phi_G(x_i, v_j))^{\frac{-1}{\beta-1}}} \quad (7)$$

The KWCM algorithm is a generalised version of the KFCM method, if the condition

$$v_k^{(t)} = \frac{\sum_{i=1}^{N} (u_{ki})^{\beta} \phi(x_i)}{\sum_{i=1}^{N} (u_{ki})^{\beta}} \quad (8)$$

is imposed [8].

On the basis of the analysis of clusters brain matter, background, cerebrospinal fluid and potential tumour or fat areas are segmented, bearing in mind the fact that fat, as well as melanin and haemoglobin, are hyperintensive even in T1-weighted images without the administration of contrast medium. The masks achieved in that way are processed with mathematic morphology operations, yielding the white and grey matter areas and thus narrowing down the region of interest. At this stage the location of lateral ventricles and eyeballs is also detected. After further automatic corrections, including the Quick Hull [13] algorithm, allowing the rejection of hypodermic fat areas, the final potential tumour areas mask is computed [8].

The local inhomogeneities of the signal intensities in the T1-weighted contrast images are responsible for uncontinuousness of the boundaries of segmented areas, which caused the need of improvement of the segmentation quality in the MS CAD by the implementation of a second segmentation step based on fuzzy connectedness. However, for the high-grade astrocytomas segmentation task, there is no such need due to the inherent presence of uncontinuousness of tumour areas caused by the necrotic tissue inside the tumour. The necrotic tissue seems to be correctly qualified by the KWCM algorithm as non-tumourous.

As already mentioned, both imaging series have the same angle positioning in coronal and saggital planes and identical location of the brain in the field of view of the images, so the perfusion maps, originnally having a 128×128 pixels resolution, may first be pre-processed with the bicubic iterpolation algorithm [16], embedded in MATLAB, to achieve the same pixel dimensions as the contrast enhanced T1-weighted images. Then they are analysed on the basis of their signal intensity.

The binary mask of hyperperfusive areas contains voxels, whose signal intensity value is more than twice the value of signal intensity of the voxels lying on the opposite side of the brain. The rough symmetry line established for this analysis is the symmetry line of the image. Finding an algorithm allowing to establish a more precise brain symmetry line will be the subject of further research.

The final tumour areas mask is calculated as the logic product of the potential tumour areas mask obtained with the KWCM algorithm and the mask of hyperperfusive regions obtained from the analysis of perfusion maps.

In the tumour areas finally obtained the number of pixels is calculated and multiplied by the MRI slice thickness plus the interslice gap, which for the contrast enhanced T1-weighted spin-echo series equal 5mm and 1.5mm respectively, yielding the final tumour volume.

3. Results

The tests have been performed on MRI data of subjects with diagnosed high-grade astrocytomas, namely one subject with GBM (subject no. 1) and two subjects with anaplastic astrocytoma (subjects no. 2 and no. 3). For one subject three consecutive MR studies were available. For each of the other subjects there was just one MR study available.

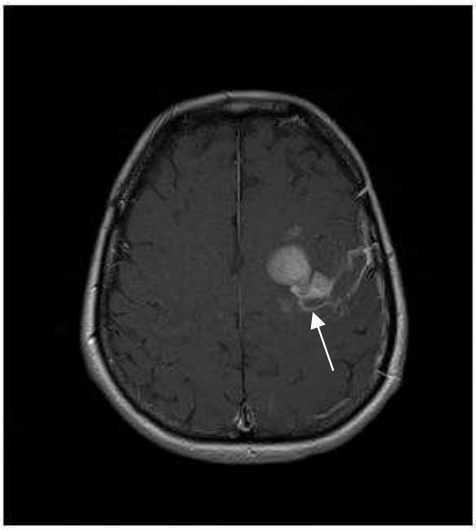

Fig. 1 Original contrast enhanced T1-weighted image selected from study no. 1 of subject no. 1.

The detailed results obtained at the subsequent steps of the segmentation algorithm are presented in Fig. 1-8. The selected images, shown in Fig. 1-4, come from the study performed after partial resection of the tumour, before radiotherapy treatment. The exclusion of the postoperative granulation tissue, indicated by an arrow on Fig. 1, from the final tumour areas mask due to the analysis of the perfusion map is well to be noted.

Fig. 2 Potential tumour areas mask obtained from the segmentation of the T1-weighted contrast image shown in Fig. 1

Radiotherapy produced a decrease in the tumour volume, although a hyperintensive area of radionecrotic tissue appears instead in the T1-weighted contrast image in Fig. 5 coming from study no. 3 of the same subject. The analysis of the corresponding perfusion map resulted in partial exclusion of the radionecrotic tissue area, indicated by an arrow on Fig. 5, from the final tumour areas mask overlying the original T1-weighted contrast image in Fig. 8. The pixels corresponding to the radionecrotic tissue area are the only false positives (FP) in the final tumour areas masks of tumour containing slices. An improvement of the algorithm of perfusion maps analysis should allow to fully exclude the radionecrotic tissue areas from the final tumour areas masks.

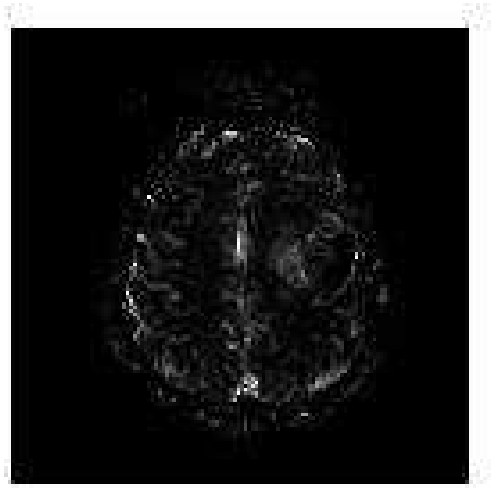

Fig. 3 Original perfusion map corresponding to the T1-weigthed contrast image in Fig. 1.

The other false positives belong to the final tumour areas masks of slices not containing the tumourous tissue. This problem might easily be overcome, if the user would interactively point out the tumour-bearing slices.

The results of automatic segmenation of brain tumours and quantification of their volume, obtained with the segmentation algorithm described in the previous section, are gathered in table 1 for all the available MR studies. Apart from the case of subject no. 2 the results achieved coincide well with the volumes as calculated by a specialised radiologist. The visual assessment of the automatically delineated brain tumours areas, performed by the radiologist, confirmed positively the coincidence of final volume results.

The tests showed that the segmentation algorithm described in the previous section does not permit to correctly classify the tumourous tissue lying close to the hypodermic fat tissue, which is the case in the T1-weighted contrast images of subject no. 2 containing the anaplastic astrocytoma. The hypodermic fat tissue rejection algorithm incorrectly classifies this lesion as fat and eliminates the region of the lesion from the final potential tumour areas mask. The development of a fat elimination algorithm enabling the correct classification of tumourous areas located closely to the fat tissue will be dealt with in further research work.

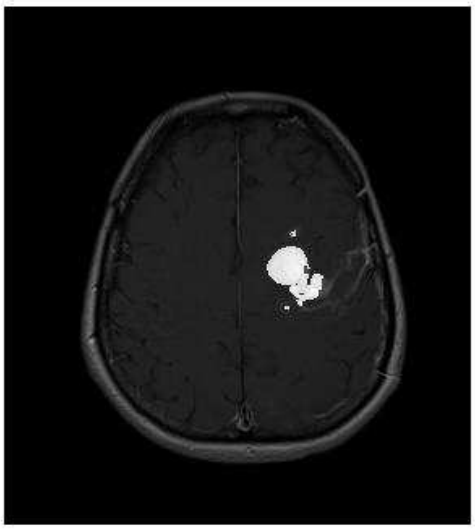

Fig. 4 Final tumour areas mask superimposed on the original contrast enhanced T1-weighted image presented in Fig. 1

Fig. 6 Potential tumour areas mask obtained from the segmentation of the T1-weighted contrast image shown in Fig. 5

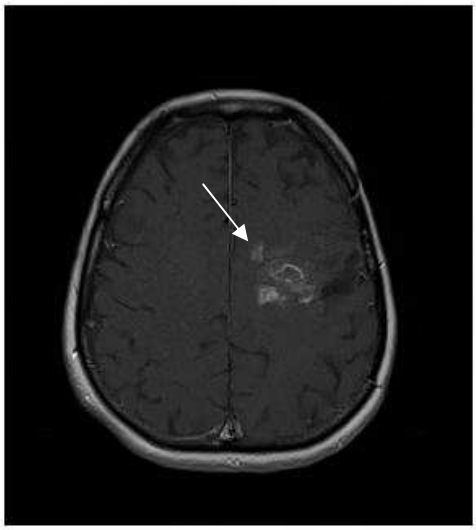

Fig. 5 Original contrast enhanced T1-weighted image selected from a follow-up study of subject no. 1

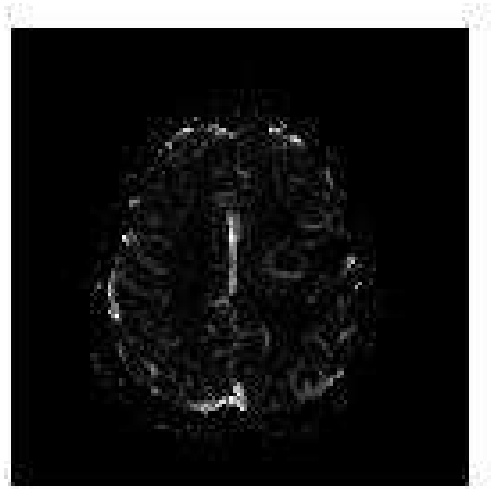

Fig.7 Original perfusion map corresponding to the T1-weigthed contrast image shown in Fig. 5

Tab.1.

Automatic Segmentation Results

Subject no.	Study no.	Brain tumour diagnosed	Tumour volume (in cm^3)
1	1	GBM	9.92
1	2	GBM	7.86
1	3	GBM	1.90
2	4	AA	-
3	5	AA	1.61

4. Conclusions

The brain tumours segmentation results achieved by using the segmentation algorithm desribed above seem to be very promising. Future work will include further improving the segmentation method and performing tests on a larger amount of imaging data of subjects with diagnosed high-grade gliomas as well as on MR images of subjects with other types of brain tumours.

5. Acknowledgement

I would like to express my gratitude to the Radiodiagnostics Department of the Maria Skłodowska-Curie Memorial Cancer Centre and

Institute of Oncology, Gliwice Branch, for making available the MRI data and medical consultation.

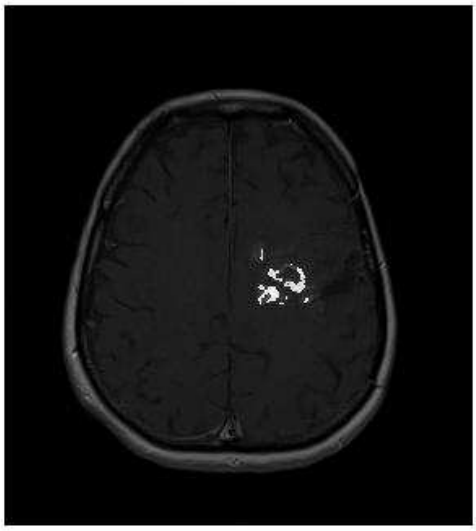

Fig. 8 Final tumour areas mask superimposed on the original T1-weighted contrast image in Fig. 5

Bibliography

[1] Brant William E., Helms Clyde A.: *Podstawy diagnostyki radiologicznej, Tom I*, Wydanie polskie, MediPage, Warszawa 2007.

[2] Runge Val M.: *Rezonans magnetyczny w praktyce klinicznej*, Elsevier Urban & Partner, Wrocław 2007.

[3] Salman Y.M. et al.: *Validation Techniques for Quantitative Brain Tumours Measurement*, Proceedings of the 2005 IEEE, Engineering in Medicine and Biology 27th Annual Conference, Shanghai, China, September 1-4, 2005.

[4] Kimmel R., Caselles V. and Sapiro G.: *Geodesic Active Contours,* International Journal on Computer Vision, vol. 1, no. 22, pp. 61-97, 1997.

[5] Zhou J. et al.: *Extraction of Brain Tumour from MR Images Using One-Class Support Vector Machine,* Proceedings of the 2005 IEEE, Engineering in Medicine and Biology 27th Annual Conference, Shanghai, China, September 1-4, 2005.

[6] Xuan X., Qingmin L.: *Statistical Structure Analysis in MRI Brain Tumour Segmentation,* Fourth International Conference on Image and Graphics, Chengdu 2007.

[7] Hongmin C.: *Probabilistic Segmentation of Brain Tumours Based on Multimodality Magnetic Resonance Images,* 4th IEEE International Symposium on Biomedical Imaging: From Nano to Macro, Washington DC 2007.

[8] Kawa J.: *Metody rozmyte w segmentacji zmian demielinizacyjnych w obrazach rezonansu magnetycznego mózgu,* Rozprawa doktorska, Politechnika Śląska, Wydział Automatyki, Elektroniki i Informatyki, Instytut Elektroniki, Gliwice 2007.

[9] Bezdek J. C.: *Pattern Recognition with Fuzzy Objective Function Algorithms,* Plenum Press, New York, 1981.

[10] Xu R. and Wunsch D.: *Survey of Clustering Algorithms,* IEEE Transactions Neural Networks, v. 16, no. 3, pp. 645-678, May 2005.

[11] Girolami M.: *Mercer Kernel-Based Clustering in Feature Space,* IEEE Transactions Neural Networks, v. 13, no. 3, pp. 780-784, May 2002.

[12] Wu Z. et al.: *Fuzzy c-Means Clustering Algorithm Based on Kernel Method,* 5th International Conference on Computational Intelligence and Multimedia Applications (ICCIMA '03), Xi'an China, IEEE 2003, pp. 49-54.

[13] Barber C. B. et al.: *The Quickhull Algorithm for Convex Hulls,* ACM Transactions on Mathematical Software, v. 22, no. 4, pp. 469-483, 1996.

[14] http://www.braintumor.org/AnaplasticAstrocytoma/

[15] http://emedicine.medscape.com/article/283453-overview

[16] Keys R. G.: *Cubic Convolution Interpolation for Digital Image Processing,* IEEE Transactions on Acoustics, Speech and Signal Processing, Vol. ASSP-29, No. 6, pp. 1153-1160, December 1981.

[17] Mekhalfa F., Goumeïdane A. B. and Nacereddine N.: *Unsupervised Algorithm for Radiographic Image Segmentation Based on the Gaussian Mixture Model*, EUROCON 2007 The International Conference on "Computer as a Tool", Warsaw, September 9-12.

[18] Zhang D. et al.: *Kernel-Based Fuzzy Clustering Incorporating Spatial Constraints for Image Segmentation,* Proceedings of the Second International Conference on Machine Learning and Cybernetics, Xi'an, 2-5 November 2003.

[19] Krex D, Klink B., Hartmann C. et al.: *Long-term survival with glioblastoma multiforme,* http://brain.oxfordjournals.org/cgi/content/full/130/10/2596

Authors:

Paweł Szwarc, MSc
Politechnika Śląska
ul. Akademicka 16
44-100 Gliwice
tel.: 032 237 17 83

email: pawel.szwarc@polsl.pl